

# Reduction of adhesive wear with use of tool coating reducing thermoelectric currents

A Schrepfer<sup>1</sup>, A Schott<sup>2</sup>, P Tröber<sup>1</sup>, M Keunecke<sup>2</sup>, M Welm<sup>1</sup>, F Steinlehner<sup>1</sup>, R Golle<sup>1</sup> and W Volk<sup>1</sup>

<sup>1</sup> Chair of Metal Forming and Casting, Technical University of Munich, 85748 Garching, Germany

<sup>2</sup> Fraunhofer Institute for Surface Engineering and Thin Films IST, 38108 Braunschweig, Germany

Agnes.Schrepfer@tum.de

**Abstract.** Blanking is one of the main processes in producing sheet metal components. The impact of adhesive wear of the blanking tools on the cost efficiency is high, especially when processing aluminum. As an influencing factor on adhesive wear in blanking, thermoelectric currents have been considered to a very small extent. Recent investigations have shown that thermoelectric currents occur in every blanking tool due to the rise of temperature in the shear zone in interaction with a difference of the material-specific Seebeck coefficients of tool and sheet metal. A reduction in the amount of wear was observed in case of a smaller difference of Seebeck coefficients and therefore lower levels of flowing thermoelectric currents. This paper follows the approach of adjusting the Seebeck coefficient of the tool material CF-H40S+ to the one of the sheet material by means of coating with CrAlN, in order to reduce the flowing thermoelectric currents and consequently adhesive wear. For this purpose, the effect of coating on the Seebeck coefficients, the thermoelectric currents during blanking as well as resulting wear quantities were investigated. Basic correlations could be revealed.

## 1. Introduction

The chemical and physical processes that take place in the contact zone of two components in interaction, leading to a progressive loss of material from the surface of a solid body are referred to as wear mechanisms [1]. Adhesive wear, as one of the most common wear mechanisms, predominates in the processing of aluminum alloys, stainless steel and titanium [2]. According to Czichos, adhesions are caused by contact between two asperities which initially deform plastically due to high surface pressure. Therefore, fragments of the protective oxide layer are pulled off and bare metallic surfaces come into contact. As the resulting chemical bonds between the contact partners are stronger than the cohesive bonds within the materials, a relative movement between the two partners causes a separation within the cohesively weaker bonded partner and a material transfer to the stronger bonded one [3]. These adhesions formed lead to a reduction in component quality. During cyclic tool engagement, material transfer builds up and consequently comes off again as sliver particles [4]. These free particles lead to an increased risk of damages of the tool, the peripheral electronics or the press [5]. Currently lubricants and coatings are used in the industrial environment to reduce adhesive wear, as they are minimizing the friction between the contact partners and therefore also the resulting frictional heat [6].

However thermoelectric currents were considered to a minor extent. While blanking, a temperature rise can be observed in the shear zone, which occurs due to three reasons: Besides macroscopic friction between tool and sheet metal and microscopic friction on an atomic level, the conversion of plastic work into heat contributes most to the temperature rise. For the aluminum alloy BS 2011, about 90 % of the



work dissipate into heat [7] and only a small portion is stored in the structure of the material [8]. Therefore, the occurring temperature is mainly influenced by the thickness and the mechanical properties of the sheet metal. It is also basic reason for the emergence of thermoelectricity during metal forming. This phenomena, called Seebeck effect, occurs when two different conductors come into contact and are subject to a temperature gradient. It leads to electric voltages that are measurable in an open circuit. In addition to the temperature gradient, the difference between the material-specific Seebeck coefficients (SCs) influences the thermoelectric voltage. The SC describes the thermoelectric behavior of materials as a measure of the increase in thermoelectric voltage depending on the temperature and is mainly influenced by the chemical composition. However, different crystal structures and grain sizes of the materials also change the SC [9]. Therefore, it must be determined experimentally for each material. In a closed conductor circuit, thermoelectric circular currents are generated due to the existing thermoelectric voltage. The strength of the current also depends on the resistance  $R$  of the entire conductor circuit [10]. Considering the temperature increase in the blanking tool, the conditions for the Seebeck effect to occur are also fulfilled during cold forming and cutting as shown in figure 1. Tool and sheet material are representing two conductors which are subject to a temperature gradient.

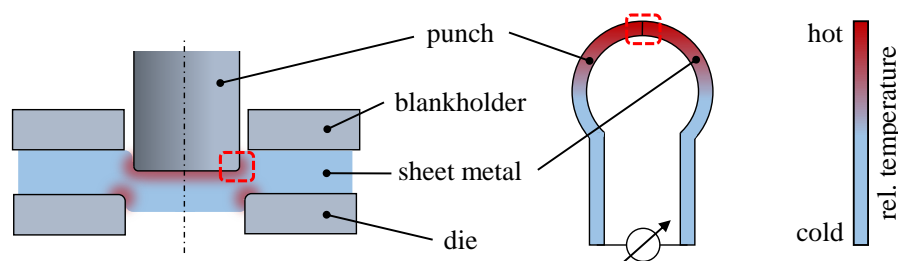


Figure 1. Schematic representation of the Seebeck effect during shear cutting [15].

At first the influence of thermoelectric currents on adhesive wear has mainly been considered in the field of machining. Several studies have shown that introducing a current that counteracts the natural thermoelectric current reduces wear and thus increases the service life of tools. In addition an insulation of the active elements in contact can also have the same effect [11]. Uehara et al. showed that the influence of tool insulation depends on the materials used [12]. Then Tröber et al. examined the influence of thermoelectric currents on the wear of tools during blanking. For this purpose, shear cutting tests were carried out with three different punch materials (1.2379, 1.4301, CF-H40S) and the sheet material EN AW 5083. A determination of the SCs showed that the stainless steel alloy 1.4301 and the sheet material have very similar coefficients values [13]. With this material combination, almost no thermoelectric current flowed between tool and sheet [14]. In contrast to the sheet material, the carbide CF-H40S has a negative SC causing the electrons to flow from punch to sheet metal. Due to the larger difference of the SCs of punch and sheet metal when using CF-H40S a larger amount of wear was formed on the punch due to the stronger thermoelectric currents in comparison to the punch out of 1.4301. However, since the SC of 1.2379 is significantly higher than that of the aluminum alloy, the direction of the current is reversed. A determination of the amount of wear showed that despite a lower current, the amount of adhesion was greater compared to the carbide punch, which showed that not only the amount but also the flow direction of the current has an influence on adhesive wear. The height and direction of the thermoelectric current and thus also the amount of wear can therefore be influenced by a suitable choice of material combinations [13]. In addition, the effects of the natural thermoelectric currents can be influenced by means of an externally controlled current, which is applied into the contact zone between the punch and the sheet [15].

In this work to reduce adhesive wear, the Seebeck coefficient of the tool material is to be adapted to that of the sheet material by means of specially developed coating in order to reduce the flowing thermoelectric current. The influence of the coating on the resulting thermoelectric current and the resulting adhesions at the punch will be investigated in experimental shear cutting tests.

## 2. Experimental Setup

### 2.1. Determination of the thermoelectric properties

For the experimental determination of SCs of conductive and solid materials a special test rig was developed at the Chair of Metal Forming and Casting [9]. A schematic sketch of the setup is shown in figure 2. Based on an integral method, the material sample is subjected to a defined temperature difference. While the one end of the sample is kept at a constant temperature of 0 °C with the aid of an ice bath, the other end is sequentially heated to 500 °C and then cooled back down to 0 °C. Thermocouples measure the temperature of the sample at each end. The warming and cooling process is carried out by contacting the sample with a copper block, which is heated by a heating cartridge and cooled again by applying compressed air and dry ice. The measurement of the arising thermoelectric voltage is recorded via two wires attached to the ends. Platinum wires with a purity of 99.99+ % are used as a reference material for the thermoelectric characterization because of its high inertness and temperature resistance. In order to minimize environmental influences on the measurement signal, the thermoelectric voltage, which is usually only in the range of  $\mu\text{V}$ , is amplified by a factor of 1000 inside the test chamber. To counteract corrosion of the materials due to the high temperatures, the entire test chamber is flooded with the inert gas argon. The SC is then calculated from the recorded thermoelectric voltage signal.

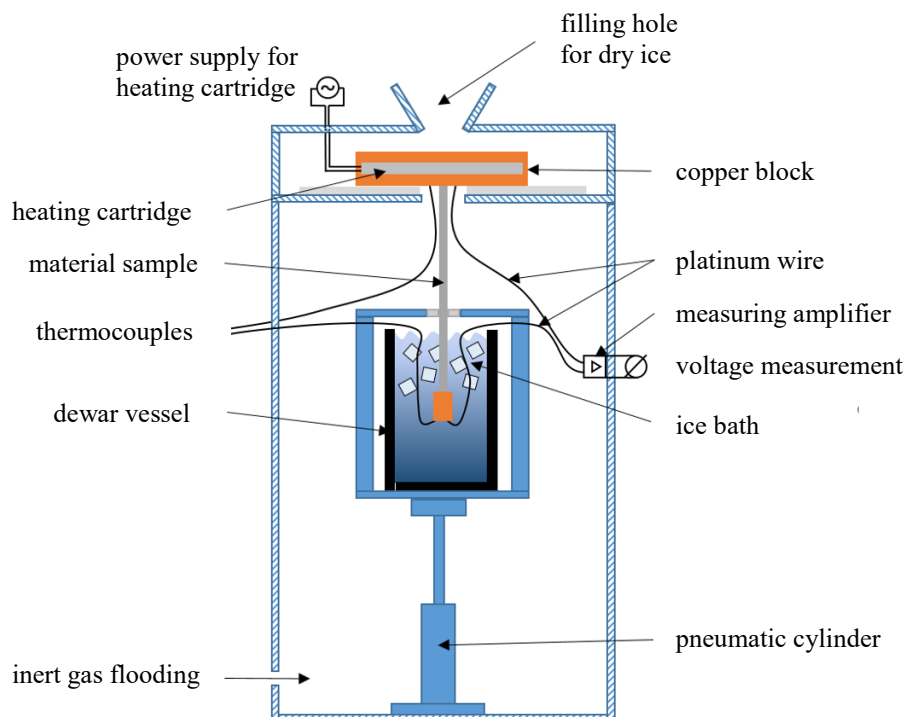


Figure 2. Test rig for the experimental determination of SCs.

### 2.2. Blanking tool and process parameters

The blanking tool for carrying out the experimental investigations has been developed specifically for measuring thermoelectricity during forming and blanking. Due to the four-track design, a simultaneous investigation of different test configurations is possible. In order to obtain accurate measurement results, both the sheet metal strip and the active elements are electrically insulated. This prevents interfering signals. To measure thermoelectric currents, a cable is attached on each punch and the sheet material, building a short circuit between them. The current flows through this connection, where a Hall probe determines both the strength and the direction of the measurable component of the thermoelectric current from the change in the electric field around the conductor. The single stroke tests were carried out on

the high performance stamping press BSTA 1600-181, Bruderer, Frasnacht (Switzerland). In order to be able to make statements about the wear status after only a few strokes an absolute cutting gap of 125  $\mu\text{m}$  was selected. With a sheet thickness of 2.5 mm, this corresponds to a relative cutting gap of 5 %. All tests were carried out with 150 strokes per minute, which corresponds to a punch impact speed of 120 mm/s, and without applying lubricants.

### 2.3. Investigated materials

The Seebeck coefficients of the tool material CF-H40S+ as well as the stainless steel material 1.4301 (X5CrNi18-10) and the aluminum alloy EN AW 5754 (AlMg3) were measured. For the investigation of the wear reduction potential of the coating, single stroke tests were carried out with the aluminum alloy. The chemical composition of these materials can be found in Table 1, 2 and 3.

Table 1. Chemical composition of 1.4301 in wt%.

	<b>C</b>	<b>Si</b>	<b>Mn</b>	<b>P</b>	<b>S</b>	<b>Cr</b>	<b>Ni</b>	<b>N</b>	<b>Fe</b>
<b>1.4301</b>	-	0.4	1.7	-	-	18.5	8.0	-	Balance

Table 2. Chemical composition of EN AW 5754 in wt%.

	<b>Si</b>	<b>Fe</b>	<b>Cu</b>	<b>Mn</b>	<b>Mg</b>	<b>Cr</b>	<b>Zn</b>	<b>Ti</b>	<b>Al</b>
<b>EN AW 5754</b>	0.1	0.3	-	0.1	3.1	0.1	-	-	Balance

Table 3. Chemical composition of CF-H40S+ in wt%.

	<b>WC</b>	<b>Co</b>	<b>Other</b>
<b>CF-H40S+</b>	86.6	11.8	-

### 2.4. Measurement of electrical resistivity

To characterize the thermoelectrical behavior of the layers, their electrical resistivity is determined by four-point measurement [16]. For this purpose, precisely defined geometries are inscribed by means of laser structuring in the layers coated on insulating substrate material. The used design can be described with width ( $w = 0.2$  mm) and length ( $l = 3.88$  mm) of the structure. Using equation 1 and 2 with thickness  $t$  of the thin film the surface resistivity  $R_{\square}$  can be determined. The electrical resistivity for thin films can be calculated with equation 3.

$$R_{\square} = \frac{\rho_{Thin\ film}}{t} \quad (1)$$

$$R_{\square} = R_{4Point} \times \frac{w}{l} \quad (2)$$

$$\rho_{Thin\ film} = R_{4Point} \times \frac{w}{l} \times t \quad (3)$$

### 2.5. Coating deposition procedure by physical vapor deposition (PVD)

Hard coatings and their modifications were deposited using a PVD magnetron sputtering system CemeCon 800/9. The system is equipped with 4 sputtering cathodes with a size of 500 mm x 88 mm and was operated in d.c. and pulsed d.c. mode. The chamber dimensions are 800 mm x 800 mm x 900 mm. The residual pressure before starting the process was  $<10^{-3}$  Pa. Prior to coating depositions substrates were cleaned with a water-based cleaning procedure. Instantly after the cleaning procedure samples were mounted into the vacuum chamber. Prior to the coating process an ion etching step with argon ions for additional surface cleaning was applied. Different coatings could be deposited by combination of different target materials on the sputtering cathodes and reactive gases like nitrogen during coating process. By varying the applied power to the sputter cathodes different coating compositions and layer sequence could be obtained. Coatings were deposited on substrates as well as ceramic plates for electrical characterization. The substrates and tools were fixed at sample holders, which are charged with a negative voltage for increased ion bombardment, and coated while rotating through the vacuum chamber.

### 3. Coating development

#### 3.1. Strategy for modification of the Seebeck coefficient by adjusting the electrical resistivity

In order to minimize the wear occurring during blanking, the pairing of the SCs of the workpiece and the tool has to be adapted to each other. For this purpose, the SC of the tool has to be modified by means of coating. The SC is a material constant and is influenced by free electrons. Consequently, the electrical conductivity respectively electrical resistivity has a significant influence on the thermoelectric properties of materials. Depending on the charge carrier density in a material, the electrical conductivity shows an opposite course to the SC. As the charge carrier concentration decreases, the SC increases. Thus, electrically insulating materials have a very high SC. [17] For the development and study of thermoelectric properties of thin films, the method of 4-point measurement for the determination of electrical resistivity was used. Due to the existing correlation of electrical conductivity and the SC, the approach is to adjust the thermoelectric properties of the thin films to the desired target range based on measured electrical resistivity by modifying the coatings structure by different phases. [18] Similar approaches are also described by [19], where the thermoelectric properties of two individual materials can be modified in combination as a nanocomposite. Most of the standard hard coating used for blanking tools, like TiN, CrN etc. have low electrical resistivities. To attain electrical resistivity and thermal conductivity in an appropriate range, such coatings has to be modified with other elements or phases. The used technique of PVD magnetron sputtering allows to deposit coatings in a wide composition range. Due to the possibility to use different target materials like Cr and Al in one coating process, it is easy to affect the coating structure and phase composition too.

#### 3.2. Development of modified CrN coatings

Very good effects for the adaptation of the SC to the sheet material were achieved by a modification of CrN coatings with aluminum respectively AlN. The specific electrical resistivity can be influenced by orders of magnitude (see table 4) by addition of AlN to CrN.

Table 4. Specific electric resistivity of applied coatings.

Coating	Specific electric resistivity [ $\Omega\text{cm}$ ]
CrN	$\sim 4.62 \times 10^{-4}$
CrAlN_1	$\sim 6.08 \times 10^{-2}$
CrAlN_2	$\sim 4.56 \times 10^{-1}$

Different CrAlN coatings were prepared by power variation of the cathodes. Due to significant different sputter rates of Cr and Al in reactive nitrogen gas mixtures three Al targets and one Cr target were used. Typical target power was between 0.5 – 2 kW per target. The negative bias voltage was in range of 30-60 V typically. The process pressure was in the range of 0.4 Pa. The analysis of the chemical composition (figure 3 a) was investigated by electron probe micro analysis (EPMA). It shows that for CrAlN\_1 an Al content of  $30 \pm 1$  at%, a Cr content of  $18 \pm 1$  at% and  $50 \pm 1$  at% nitrogen was obtained. For CrAlN\_2 an Al content of  $35 \pm 1$  at%, Cr content of  $11 \pm 1$  at% and  $50 \pm 1$  at% nitrogen was measured. By reducing the Cr content and simultaneously increasing the Al content the electrical resistivity was enhanced by an order of magnitude from appr.  $10^{-2} \Omega\text{cm}$  to the range of  $10^{-1} \Omega\text{cm}$  (figure 3 b). Because of pure Al and Cr target materials with nitrogen as reactive gas were used for coating deposition, it is reasonable that the coating structure is affected by the rotational movement of the tools through the vacuum chamber and along different coating material and resulting in a layered coating structure of alternating AlN rich and CrN rich layers. These coating structure of multilayers or nanolayers for modified nitride coatings is comparable with the developments of modified nitride hard coatings for nanostructured high-performance tool coatings [20]. Therefore, this approach seems to be promising for blanking tools coatings as well. Due to the fact that relative high Al contents are needed to attain the desired electrical resistivity range and thus the SC, it is recommended to use combinations of AlCr-mixture and Al-targets for coating deposition. For TiAlN coatings the use of mixture or alloyed targets

provide good and well adherent hard coatings for tools [21] but lower specific electrical resistivity values compared to CrAlN (figure 3 b).

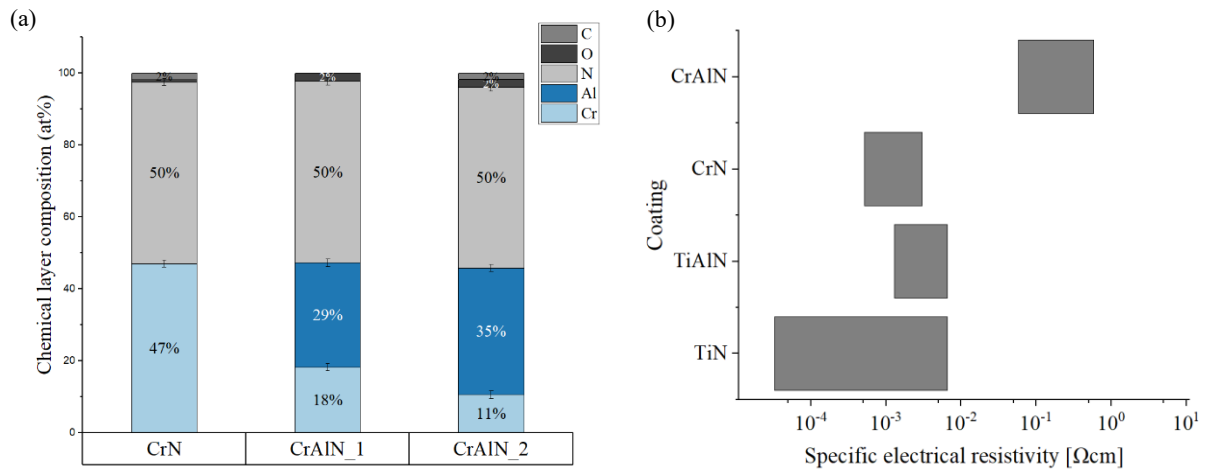


Figure 3. a) Chemical composition results of EPMA analysis for CrN and modified CrAlN layers b) Specific electrical resistivity of different hard coatings.

In combination with an adapted pre-treatment and surface finish of the blanking tools it should be possible to increase the coating performance and maintain the desired electrical resistivity and SC range. Furthermore it could be possible to adjust the coating resistivity and SC to the tool and workpiece material. For this purpose further development work is needed.

## 4. Results and Discussion

### 4.1. Seebeck coefficients of carbide before and after coating and of selected sheet materials

The SC of CF-H40S+ is negative in the temperature range from 0 °C to 300 °C due to the high cobalt content. In comparison, the SCs of the sheet materials EN AW 5754 and 1.4301 are positive, resulting in a high difference in the SCs of the sheet and the uncoated tool material as shown in figure 4 a. By means of coating with CrAlN, the SC difference between the carbide and the sheet material can be significantly reduced. Best results were obtained using the chemical composition of the CrAlN\_1-layer (see 3.2), which is also shown in figure 4 a as a layer on CF-H40S+. A concomitant reduction in the

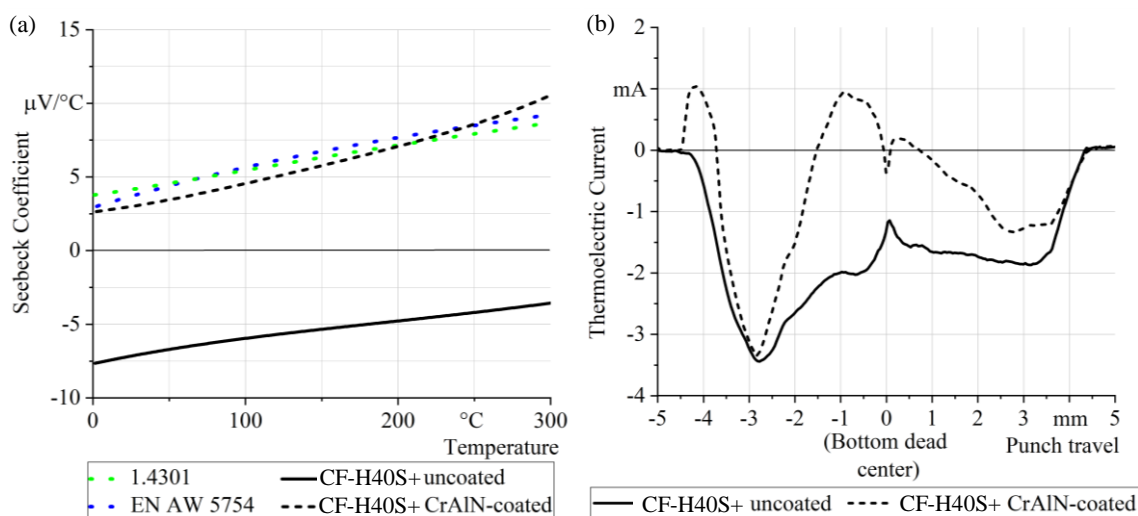


Figure 4. a) Seebeck coefficients of CF-H40S+ uncoated and CrAlN-coated, EN AW 5754 and 1.4301 b) Thermoelectric currents over punch travel for CF-H40S+ uncoated and CrAlN-coated while cutting EN AW 5754.

amount of adhesions on the punch should therefore be possible with the use of this coating with regard to literature.

#### 4.2. *Impact of Seebeck coefficients on thermoelectric currents*

Figure 4 b shows the course of the measured thermoelectric currents averaged over 9 strokes when blanking the aluminum alloy EN AW 5754. It can be seen that the maximum thermoelectric current, flowing between sheet and punch, has a negative sign, which by definition corresponds to an electron flow from punch to sheet metal. At the beginning of the contact between the punch and the sheet metal, the current increases as the punch travel progresses until the moment of crack formation in the sheet metal. Afterwards, it decreases until the bottom dead centre is reached. When the punch movement is reversed, the current rises again slightly until it drops to zero when the punch leaves the punching grid. The maximum absolute value of the averaged thermoelectric current in case of an uncoated punch is -3.49 mA. Due to the change in SC (figure 4 a), a reduction in the flowing current is possible when a CrAlN layer is used. It can be seen, that as well as at the beginning and near the bottom dead center the thermoelectric current showed even positive values, at the exact bottom dead center it drops back into negative values. This can be attributed to the fact that when measuring the SC, a slow heating of the entire sample takes place over a larger volume, resulting in a greater influence of the base material. During blanking, the temperature in the shear zone increases rapidly, which mainly heats the layer and the layer material thus dominates in terms of the SC. Therefore, the SC of the CrAlN-coated punch is higher than that of the sheet material at higher temperatures, resulting in reversed current directions. A shift of the current curves in a positive direction over a great part of the punch travel can be observed. However at a punch position of -3 mm, the absolute maximum values of both punches are in a similar range. This can be attributed to the fact that the coating started to peel off from the stamp surface. Since the adhesion of the coating fails primarily at the cutting edge of the punch, as it is case with most coatings used in industry, similarly high thermoelectric currents can be measured during the cutting process. When the cutting process is finished and the cutting edge loses contact with the sheet metal, there is only contact between the coated lateral surface of the punch and the sheet metal. During this phase and the return stroke, the effects of the changed Seebeck coefficient are clearly visible in the thermoelectric current curve.

#### 4.3. *Thermoelectric currents and adhesive wear*

Conclusions about the amount of adhesion that has been formed on the punch over the first 9 strokes can be drawn by looking at the recorded punch force. Figure 5 a shows the measured punch force during stroke 1, stroke 5 and stroke 9 over the punch travel while cutting EN AW 5754. All curves show a rapid increase when the punch hits the sheet metal at -4.1 mm, a sharp drop in the force when cracks occur and a force required to push the slug through the die channel at -1.5 mm to 0 mm. During the return stroke tensile forces act on the punch in opposite direction, which indicate friction between punch and punching grid. When the punch leaves the punching grid, the force reaches a value of zero. It can be seen, that maximum force, push through force and pull back force are higher when using the CrAlN-coated punch which can be attributed to the higher surface roughness of the coated punch. A comparison of the maximum push-through force and the maximum retraction force after stroke 1 and stroke 9 shows that both forces increase with the number of strokes performed. This indicates that the amount of adhesion on the punch increases noticeably, causing high friction. A thermal expansion of the punch can be excluded, as the individual strokes were performed with a time interval of several minutes. Comparing the punch force curves from 1 to 9 strokes in figure 5 b gives indication of the wear-reducing effect of the CrAlN coating. An increase in the push-through force and retraction force is significantly less pronounced here than with the previously considered uncoated punch.

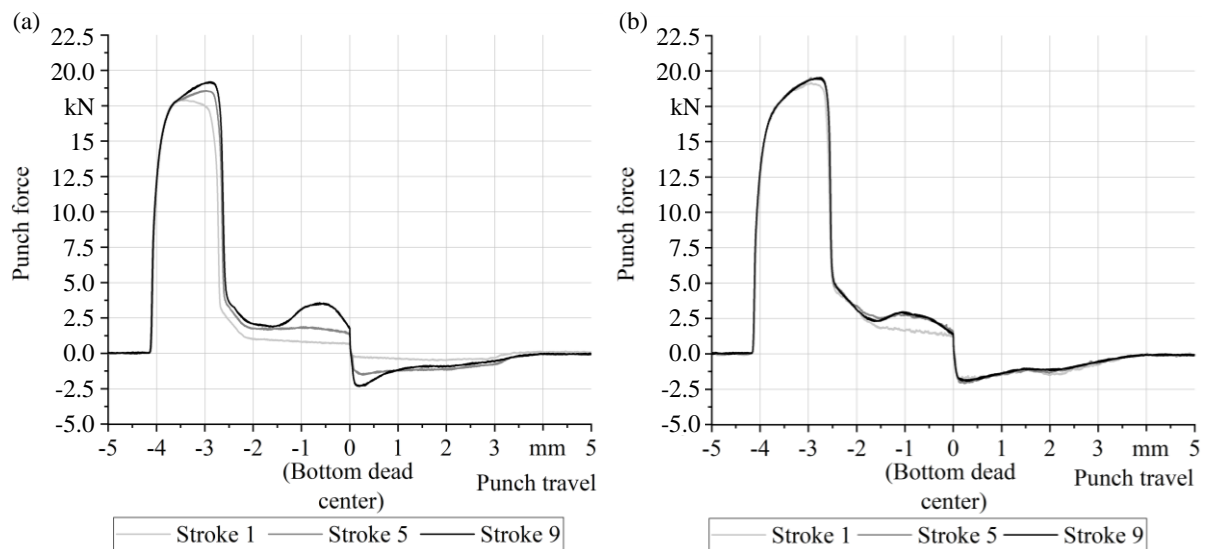


Figure 5. Punch forces over punch travel for CF-H40S+ (a) uncoated and (b) CrAlN-coated when cutting EN AW 5754.

The assumption of a reduced amount of adhesive material transfer with CrAlN-coated punch is confirmed when comparing the punch surfaces before the first stroke and after the ninth stroke. Using a laser microscope, the punches worn lateral surface was recorded in at least four locations evenly distributed around the circumference, where an area with a width of 1 mm was recorded. For analysing the wear quantity the curvature of the punch was compensated and the adhesive wear volume was measured. In order to exclude the influence of manufacturing disparities, the material volume resulting from the surface roughness was subtracted. Finally, the wear coefficient is calculated by dividing the remaining volume by the surface area under consideration. Therefore, the wear coefficient indicates the height of transferred material assuming an even distribution. Already after nine strokes, a formation of adhesions on the uncoated punch surface is clearly visible. An evaluation of the height of the adhesions on the punch surface revealed a wear coefficient (VQ) of  $0.35 \mu\text{m}$ . In contrast, the laser microscope measurements of the punch surface of the CrAlN-coated punch after 9 strokes in figure 6 show only slight wear. An evaluation of the wear coefficient resulted in a value of  $0.21 \mu\text{m}$ , which represents 60 % of the amount of adhesions of the uncoated punch. A close look at the surface of the CrAlN-coated punch shows that the coating started to detach as the recorded thermoelectric currents suggested, therefore, the adhesion of the coating needs to be further improved for use in an industrial environment.

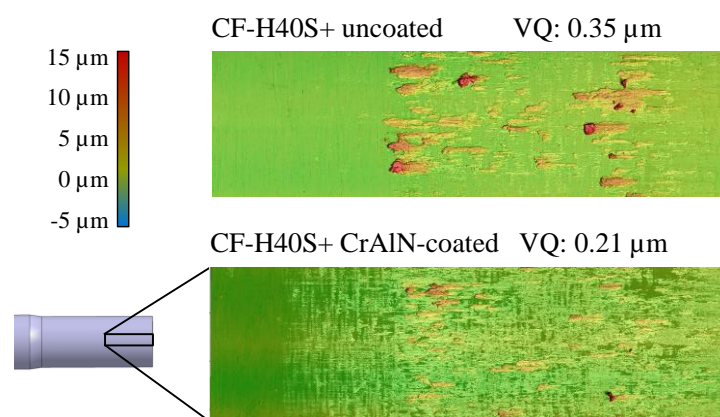


Figure 6. Laser microscopic pictures of the adhesive wear distribution on the punches lateral surface after cutting EN AW 5754.

In order to be able to exclude an influence of the temperature development in the shear zone as well as different friction conditions between punch and sheet metal as a possible reason for the reduced thermoelectric currents, the cutting surfaces of the punching grids were also considered. Figure 7 shows the individual zones of a characteristic shear cut surface. While cutting at first the roll over and clean-cut form. With advancing punch position material failure begins and the sheet metal tores. The torn zone and the burr arise. Figure 8 shows that the CrAlN-coated punch leads to a higher proportion of clean-cut with 57 % in comparison to 45 % of clean-cut using the uncoated punch. This shows that cracking occurs earlier with progressive punch stroke in the uncoated punch, suggesting that the temperatures in the shear zone are lower here. Thus, although the temperatures in the shear zone are higher with the CrAlN-coated punch, the thermoelectric current was lower and so were the resulting amounts of adhesions to the punch. A lower measured thermoelectric current when using the CrAlN-coated punch is therefore due to the adjusted Seebeck coefficient. Likewise, the surface of the clean-cut after only one stroke is significantly rougher when using the CrAlN-coated punch than when using an uncoated punch, because of the higher roughness of the coated punch. Although the higher roughness normally leads to higher adhesions on the punch due to the surface pressure, lower adhesions were measured here. This improvement can therefore also be attributed to the Seebeck coefficient.

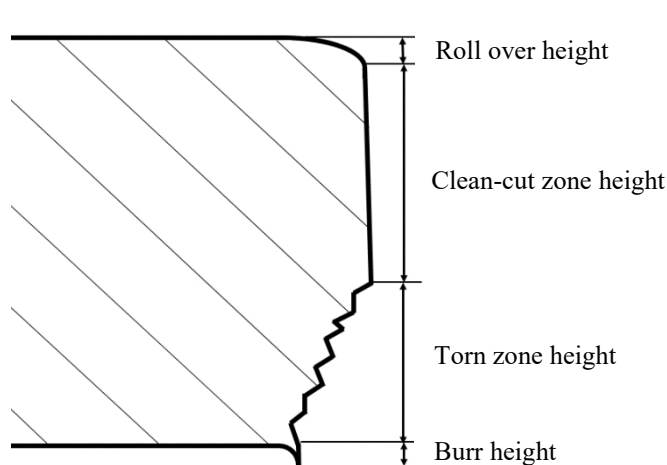


Figure 7. Cutting surface characteristic values.

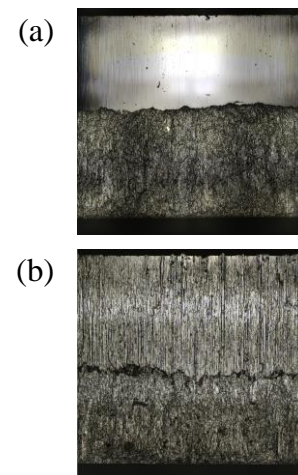


Figure 8. Cutting surface of EN AW 5754 after cutting with (a) uncoated and (b) CrAlN-coated punch.

## 5. Conclusion

In this paper, it could be shown that it is basically possible to influence and adjust the Seebeck coefficient by a coating and its modification respectively. By adjusting the Seebeck coefficient of the tool material to the one of the sheet metal, the flowing thermoelectric current and consequently the amount of adhesive wear could be reduced. Furthermore, the findings will help to improve the understanding of the wear causing interactions. The improvement of the mechanical coating properties as well as its adhesion will be part of future projects.

## Acknowledgement

The authors would like to thank the German Federation of Industrial Research Associations (AiF) for the financial support under the grant number 20693N.

## References

- [1] Czichos H and Habig K-H 2010 *Tribologie Handbuch – Tribometrie, Tribomaterialien, Tribotechnik* (Wiesbaden: Vieweg + Teubner-Verlag) pp 117-30
- [2] Groche P, Nitzsche G and Elsen A 2008 Adhesive wear in deep drawing of aluminum sheets

- Annals of the CIRP* **57** pp 295-8.
- [3] Buckley D H 1981 Surface effects in adhesion, friction, wear and lubrication *Elsevier Tribology Series* **5**
- [4] Krinninger M, Steinlehner F, Opritescu D, Golle R and Volk W 2017 On the influence of different parameters on the characteristic cutting surface when shear cutting aluminum *Procedia CIRP* **63** pp 230-5
- [5] Schilp H, Hoffmann H, Golle R and Hoogen M 2004 Flitterreduzierung beim Schneiden von Aluminiumblech *Blech Rohre Profile* **51**, pp 78-9
- [6] Schulz J, Brinksmeier E, Meyer D and Schultalbers M 2015 Vertiefende Untersuchungen zu Verschleißschutzadditiven und deren Wechselwirkung mit Metalloberflächen *56. Tribologie-Fachtagung GfT-Tagungsband*
- [7] Macdougall D 2000 Determination of the plastic work converted to heat using radio-metry *Experimental Mechanics* **40/3** pp 298-306.
- [8] Demmel P, Hoffmann H, Golle R, Intra C, Volk W 2015 Interaction of heat generation and material behaviour in sheet metal blanking *Annals of the CIRP* **64**, pp 249-52
- [9] Demmel P, Tröber P, Kopp T, Golle R, Volk W and Hoffmann H 2013 Characterization of the thermoelectric behavior of plastically deformed steels by means of relative Seebeck coefficient *Materials Science Forum* **755** pp 1-7
- [10] Barnard R D 1972 *Thermoelectricity in metals and alloys*
- [11] Shan H and Pandey P 1975 Wear of Cutting Tools: Thermoelectric effects *Wear* **32** pp 167-79
- [12] Uehara K, Sakurai M and Ikeda T 1992 On the problem of thermoelectric current in metal cutting *Annals of the CIRP* **41** pp 75-8
- [13] Tröber P, Demmel P, Hoffmann H, Golle R and Volk W 2017 On the influence of Seebeck coefficients on adhesive tool wear during sheet metal processing *CIRP Annals* **66/1** pp 293-6
- [14] Welm M, Tröber P, Weiss H, Demmel P, Golle R and Volk W 2020 Thermoelectrically based approaches to reduce adhesive wear during blanking *JOM* **72/7** pp 2025-35
- [15] Tröber P, Weiss H A, Kopp T, Golle R and Volk W 2017 On the correlation between thermoelectricity and adhesive tool wear during blanking of aluminum sheets *International Journal of Machine Tools and Manufacture* **118-119** pp 91-7
- [16] Chen X, Dai W, Wu T, Luo W, Yang J, Jiang W and Wang L 2018 Thin film thermoelectric materials: Classification, characterization, and potential for wearable applications *Coatings* **8** p 244
- [17] Rowe D M 2006 *Thermoelectrics handbook: Macro to nano* (CRC Press Taylor & Francis Group)
- [18] Gharavi M A, Kerdsonpanya S, Schmidt S, Eriksson F, Nong N V, Lu J, Balke B, Fournier D, Belliard L and le Febvrier A 2018 Microstructure and thermoelectric properties of CrN and CrN/Cr2N thin films *Journal of Physics D: Applied Physics* **51/53**
- [19] Dehkordi A M, Zebarjadi M, He J and Tritt T M 2015 Thermoelectric power factor: Enhancement mechanisms and strategies for higher performance thermoelectric materials *Materials Science & Engineering R* **97** pp 1-22
- [20] Stein C 2016 Entwicklung von nanostrukturierten Nitriden und c-BN als Verschleißschutzschichten für Zerspanwerkzeuge (Stuttgart: Fraunhofer Verlag) **160**
- [21] M. Keunecke et al 2010 Modified TiAlN coatings prepared by d.c. pulsed magnetron sputtering *Surface & Coatings Technology* **205** pp 1273-8